Detrend-Free Hemodynamic Data Assimilation of Two-Stage Kalman Estimator

Hu Zhenghui[1] and Shi Pengcheng[2]

[1] State Key Laboratory of Modern Optical Instrumentation, Zhejiang University, Hangzhou 310027, China
[2] B. Thomas Golisano College of Computing and Information Sciences, Rochester Institute of Technology Rochester, NY 14623, USA
zhenghui@zju.edu.cn

Abstract. Spurious temporal drift is abundant in fMRI data, and its removal is a critical preprocessing step in fMRI data assimilation due to the sparse nature and the complexity of the data. Conventional data-driven approaches rest upon specific assumptions of the drift structure and signal statistics, and may lead to inaccurate results. In this paper we present an approach to the assimilation of nonlinear hemodynamic system, with special attention on drift. By treating the drift variation as a random-walk process, the assimilation problem was translated into the identification of a nonlinear system in the presence of time varying bias. We developed two-stage unscented Kalman filter (UKF) to efficiently handle this problem. In this framework the assimilation can implement with original fMRI data without detrending preprocessing. The fMRI responses and drift were estimated simultaneously in an assimilation cycle. The efficacy of this approach is demonstrated in synthetic and real fMRI experiments. Results show that the joint estimation strategy produces more accurate estimation of physiological states, fMRI response and drift than separate processing due to no assumption of structure of the drift that is not available in fMRI data.

1 Introduction

Over the past decade, the neuroimaging community has witnessed an explosive rise in research that melds observed fMRI data with hemodynamic response models to generate accurate forecasts on underlying physiological states and/or parameters [4,6]. In general, a comprehensive assimilation scheme is suitable for most nonlinear phenomena and distinct spatio-temporal scales. Even though the modeling may differ, the approach chosen is general [9].

However, there is still something unique to fMRI data that needs additional concern. The original fMRI measurements contain abundant slowly varying drift. These undesirable drift may be caused by instrumental instability, spontaneous head movement, as well as aliasing of physiological pulsations. The amount and direction of drift is difficult to predict, whereas estimation and removal of these components have a strong impact on assimilation performance and ensuing statistical analysis due to the inherent low signal to noise ratio (SNR) of fMRI

G. Fichtinger, A. Martel, and T. Peters (Eds.): MICCAI 2011, Part II, LNCS 6892, pp. 242–250, 2011.

data. And, from a frequency perspective, the nuisance drift is also difficult to be discriminated from *true* fMRI response that often has similar low frequency components. Detrending therefore is an important preprocessing step in fMRI data analysis.

Although the conventional data driven methods have provided good performance, and there have been numerous attempts on drift function design and optimization for their improvement, it remains true that all data-driven detrending methods are based on specific assumptions of the drift curve and signal statistics [1]. In practice, however, the drift has complicated structures due to the interaction of various possible sources. Real drift is noisy, not a smooth curve supposed by data driven methods. In this context, such assumptions may not capture the structure of drift well. As a result, the quality of the assimilation will be subject to degradation imposed by these assumption on drift formulation.

Since the assimilation processing always occurs in activation areas, the actual trended fMRI signal can be explained as a linear combination of the hemodynamic response and drift. Considering a more general case, in which both process and observation are biased,

$$\dot{\mathbf{x}} = f(\mathbf{x}, \boldsymbol{\theta}) + \mathbf{B}\mathbf{b} + \mathbf{v} \qquad \mathbf{v} \sim N(0, \mathbf{Q}) \tag{1}$$

$$\mathbf{y} = h(\mathbf{x}, \boldsymbol{\theta}) + \mathbf{C}\mathbf{b} + \mathbf{w} \qquad \mathbf{w} \sim N(0, \mathbf{R}) \tag{2}$$

where f is nonlinear hemodynamic response function, h is nonlinear measurement function that describes the transformation from physiologic states to the fMRI observation at a given brain region, $\mathbf{x}$ represents physiological state, $\boldsymbol{\theta}$ is physiological parameters, $\mathbf{B}$, $\mathbf{C}$ are time-variant coefficient matrices. $\mathbf{b}$ is biases state and $\mathbf{y}$ is the measurement. The process and measurement noise $\mathbf{v}$,$\mathbf{w}$ are zero-mean white Gaussian noise. It is noted that the drift is low frequency, slowly varying component, and can be treated as stochastic variation in assimilation procedure. In this sense, the assimilation problem naturally fall into the problem of estimating the state variables of a nonlinear system in the presence of unknown random bias.

Eq. (1) and (2) form a state-space-like representation for the fMRI data assimilation problem, with (1) describing the physiological process and (2) expressing the observation. However, the bias terms make the problem in a nonstandard state-space formulation. A convenient approach to this problem is to concatenate the original state vector and the bias terms into a higher-order state vector. The filter then implements on the augmented state space. However, it may suffer from computational burden and numerical problems when state dimensions are large because of solving the inverse of the covariance matrix. This method therefore is reasonably effective only when the number of states is relatively small. In 1969, Friedland introduced a Kalman estimation concept applicable to the case in which state variables contain unknown, constant bias [3]. The resulting two-stage estimator has since received considerable attention because of its inherent computational efficiency and stability. It was also extended to handle nonlinear

systems and more general cases (e.g. time varying bias) [5]. However, most of them cast the standard extended Kalman filter (EKF) into a two-stage structure to deal with nonlinearity, therefore easily lead to the problem of numerical stability due to the linearization of the nonlinear system in practical application and their method is reliable only for near linear system on the time scale of the updates. The unscented Kalman filter (UKF) has been developed to address the deficiencies of EKF [8]. In this paper, we develope a two-stage unscented Kalman estimator for the nonlinear system in the presence of unknown random bias. In this framework, the fMRI response, system states associated with physiological variables and the drift can be forecasted at the same assimilation procedure, thereby realizing detrend-free assimilation approach to original fMRI data without detrending preprocessing.

2 Unscented Kalman Estimator

Two-stage estimation separates the estimation of the bias from that of the dynamic state, thereby reducing the dimensionality of states involved in the computations. Two separate, uncoupled filter run in parallel to generate the optimal estimate of the bias and of the "bias-free" state. A thorough description of the linear two-stage estimator can be found in (not presented here for lack of space) [3]. For a nonlinear dynamic system, the bias-free estimator can be immediately replaced with the standard UKF formulation [8]:

$$\mathcal{X}_{k-1} = [\hat{\mathbf{x}}_{k-1}\ \hat{\mathbf{x}}_{k-1} + \eta\sqrt{\mathbf{P}_{k-1}}\ \hat{\mathbf{x}}_{k-1} - \eta\sqrt{\mathbf{P}_{k-1}}] \tag{3}$$

$$\mathcal{X}_{k|k-1} = F[\mathcal{X}_{k-1}, \mathbf{u}_{k-1}] \tag{4}$$

$$\hat{\mathbf{x}}_k^- = \sum_{i=0}^{2L} W_i^{(m)} \mathcal{X}_{i,k|k-1} \tag{5}$$

$$\mathbf{P}_k^- = \sum_{i=0}^{2L} W_i^{(c)} [\mathcal{X}_{i,k|k-1} - \hat{\mathbf{x}}_k^-][\mathcal{X}_{i,k|k-1} - \hat{\mathbf{x}}_k^-]^T + \mathbf{R}^{\mathbf{v}} \tag{6}$$

$$\mathcal{Y}_{k|k-1} = \mathbf{H}[\mathcal{X}_{k|k-1}] \tag{7}$$

$$\hat{\mathbf{y}}_k^- = \sum_{i=0}^{2L} W_i^{(m)} \mathcal{Y}_{i,k|k-1} \tag{8}$$

$$\mathbf{P}_{\tilde{\mathbf{y}}_k \tilde{\mathbf{y}}_k} = \sum_{i=0}^{2L} W_i^{(c)} [\mathcal{Y}_{i,k|k-1} - \hat{\mathbf{x}}_k^-][\mathcal{Y}_{i,k|k-1} - \hat{\mathbf{y}}_k^-]^T + \mathbf{R}^{\mathbf{n}} \tag{9}$$

$$\mathbf{P}_{\mathbf{x}_k \mathbf{y}_k} = \sum_{i=0}^{2L} W_i^{(c)} [\mathcal{X}_{i,k|k-1} - \hat{\mathbf{x}}_k^-][\mathcal{Y}_{i,k|k-1} - \hat{\mathbf{y}}_k^-]^T \tag{10}$$

$$\mathcal{K}_k = \mathbf{P}_{\mathbf{x}_k\mathbf{y}_k}\mathbf{P}^{-1}_{\tilde{\mathbf{y}}_k\tilde{\mathbf{y}}_k} \tag{11}$$

$$\hat{\mathbf{x}}_k = \hat{\mathbf{x}}^-_k + \mathcal{K}_k(\mathbf{y}_k - \hat{\mathbf{y}}^-_k) \tag{12}$$

$$\mathbf{P}_k = \mathbf{P}^-_k - \mathcal{K}_k\mathbf{P}_{\tilde{\mathbf{y}}_k\tilde{\mathbf{y}}_k}\mathcal{K}^T_k \tag{13}$$

having the following variable definitions: $\mathbf{P}$ is the covariance matrix, $\alpha = 0.01$ determines the size of the sigma-point distribution, $\beta = 2$ for a Gaussian distribution, L is the states dimension, $\lambda = L(\alpha^2 - 1)$ and $\eta = \sqrt{(L + \lambda)}$ is the scaling parameter, $\{W_i\}$ is a set of scalar weights ($W^{(m)}_0 = \lambda/(L + \lambda)$, $W^{(c)}_0 = \lambda/(L + \lambda) + (1 - \alpha^2 + \beta)$, $W^{(m)}_i = W^{(c)}_i = 1/\{2(L + \lambda)\}$, $i = 1,\ldots,2L$). $\mathbf{R_v}$, $\mathbf{R_n}$ is the process and observation noise. The recursive algorithm given by (3-13) defines the first stage of a two-stage estimator.

The bias b is time-varying term added to nonlinear functions. It is clear that the bias estimator have the same forms as in the original linear separate-bias estimation. It is realized in another separate recursive procedure:

$$\hat{b}^-_k = \hat{b}^-_{k-1} \tag{14}$$

$$P^-_b(k) = P_b(k - 1) \tag{15}$$

$$K_b(k) = P^-_b(k)S^T_k[H_k\mathbf{P}^-_k H_k + S_k P^-_b(k)S^T_k + R_n]^{-1} \tag{16}$$

$$P_b(k) = [I - K_b(k)S_k]P^-_b(k) \tag{17}$$

$$\hat{b}_k = \hat{b}^-_k + K_b(k)(r_k - S_k\hat{b}^-_k) \tag{18}$$

where $\hat{b}$ is the bias estimate, K_b is the bias gain equation, P_b is the bias estimation error covariance matrix, $r_k = \mathbf{y}_k - \hat{\mathbf{y}}^-_k$ is the measurement residual of the bias-free estimation, r_k and $\mathbf{P}^-_k$ can be available from the bias-free estimator, and S_k is available from the sensitivity functions.

Note that $H_k\mathbf{P}^-_k H_k$ is the measurement covariance, by the definitions given by Equation (9), Equation (16) becomes

$$K_b(n) = P^-_b(n)S^T_n[\sum_{i=0}^{2L} W^{(c)}_i[\mathcal{Y}_{i,k|k-1} - \hat{\mathbf{x}}^-_k][\mathcal{Y}_{i,k|k-1} - \hat{\mathbf{y}}^-_k]^T + S_n P^-_b(n)S^T_n + R_n]^{-1} \tag{19}$$

The recursive algorithm defined by (14–15) and (17–19) constitute the second stage of the two-stage Kalman estimator.

Suppose that the bias is perfectly known, the optimal estimate of b would be the constant value, and the recursive estimate of x may be expressed as

$$\hat{X}_k^- = f(\hat{x}_{k-1}) + B_k b \tag{20}$$

$$\hat{X}_k = \hat{X}_k^- + \mathcal{K}_k(y_k - h(\hat{X}_k^-) - C_k b) \tag{21}$$

where $\hat{X}_k^-$ and $\hat{X}_k$ are the *priori* and *posteriori* estimates of x when b is perfectly known, and b is the true value of the bias vector. Its gain equation is clearly identical to that of the bias-free estimator. Since the bias term is linear in nature, the component of the general X estimate due to the forcing function y is identical to the bias-free x estimate. It allows the following relationship as given [3]:

$$\hat{X}_k^- = \hat{x}_k^- + U_k b \tag{22}$$

$$\hat{X}_k = \hat{x}_k + V_k b \tag{23}$$

where U and V is *priori* and *posterior* sensitivity functions, respectively. The key step for developing the bias aware nonlinear estimator is to design the sensitivity functions, which connect two parallel filters. From Equation (22), we have

$$\hat{X}_k^- - \hat{x}_k^- = f(\hat{X}_{k-1}) - f(\hat{x}_{k-1}) + B_k b = \left(\left. \frac{\partial f}{\partial x} \right|_{x=\hat{x}_{k-1}} V_{k-1} + B_k \right) b \tag{24}$$

Therefore, a *priori* sensitivity function becomes

$$U_k = \left. \frac{\partial f}{\partial x} \right|_{x=\hat{x}_{k-1}} V_{k-1} + B_k \tag{25}$$

Similarly, the posterior error is written as

$$\hat{X}_k - \hat{x}_k = V_k b = \left[U_k - \mathcal{K}_k \left(\left. \frac{\partial h}{\partial x} \right|_{x=\hat{x}_k^-} U_k + C_k \right) \right] b \tag{26}$$

The a *posterior* sensitivity becomes

$$V_k = U_k - \mathcal{K}_k S_k \tag{27}$$

where S_k is given by

$$S_k = \left. \frac{\partial h}{\partial x} \right|_{x=\hat{x}_k^-} U_k + C_k \tag{28}$$

Equations (25), (27), and (28) develop as the counterpart of the sensitivity functions in the linear bias aware estimation. Taken together they provide a recursive algorithm, which links two separate stages. Thus, it is possible to employ the estimate of b for correcting the bias-free estimate $\hat{x}$ in the nonlinear bias system. The optimal estimate output give as (22) (23).

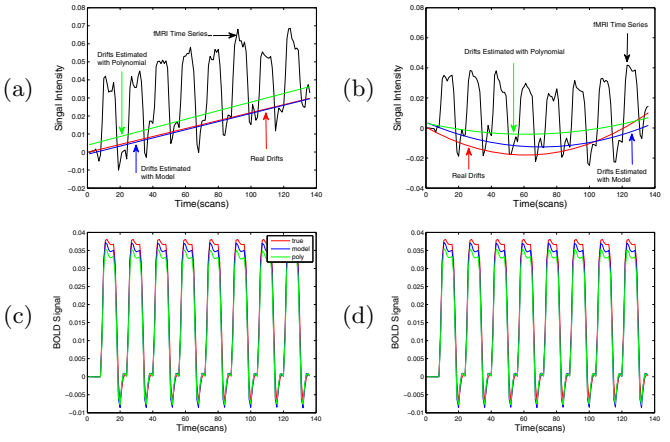

Fig. 1. Estimated drift (a,b) and fMRI signal (c,d) from synthetic data with linear drift and quadratic drift

3 Experimental Validation and Discussion

We consider the actual fMRI measurements in which only the observations are biased, $\mathbf{B} = 0$. The physiological processes underlying the BOLD response were charactered using the hemodynamic Balloon model in this study [2,4]. The resting blood volume fraction $V_0 = 0.02$ [6] and stiffness parameter $\alpha = 0.33$ are assumed known [7] in the assimilation procedure.

Synthetic Data. Since the ground truth is unavailable in real fMRI data, synthetic data are chosen to examine the proposed approach. The synthetic time series contains a known activation response, a known drift term b_j, and Gaussian white noise e_j, with signal-to-noise ratio (SNR) of 3dB. We implement linear drift and quadratic drift in the experiment. The artificial BOLD response is generated by Balloon model, where $\epsilon = 0.59$, $\tau_s = 1.38$, $\tau_f = 2.7$, $\tau_0 = 0.89$, $\alpha = 0.33$, $E_0 = 0.3$, and $V_0 = 0.02$ within their typical range [4]. The experimental condition of synthetic data is consistent with real fMRI experiments below.

Figure 1 (a), (b) show the synthetic time series and the known and estimated drift by the proposed method and the polynomial method [1]. The hemodynamic response of detrend-free assimilation, assimilation after polynomial detrending and true response are shown in Figure 1 (c), (d). Polynomial detrending generates an elevated drift estimate due to the whitening assumption. The recalibration of the baseline can only partly alleviate this effect, shown as a green line in Figure 1. The artificial elevated drift result in underestimated fMRI response (green line), and degrade the performance of data assimilation. In contrast, with the constraint of the hemodynamic model, our two-stage assimilation strategy tracks the known drift better, illustrating the advantage of introducing physiologically meaningful prior into detrending. As a result, the two-stage assimilation

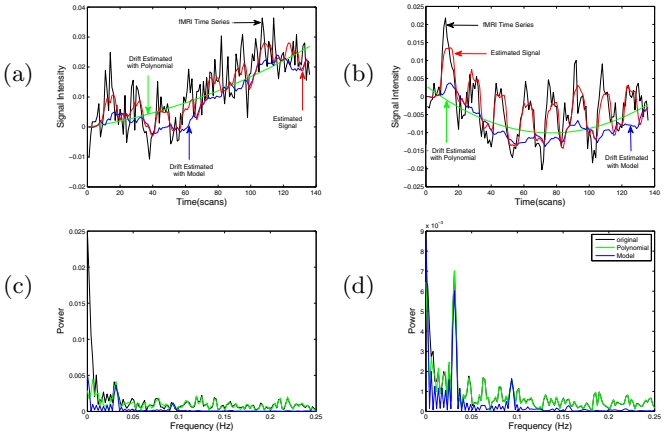

Fig. 2. Real fMRI signal and estimated drifts (a,b), as well as their spectra (c,d)

Subject	F-Statistics ($F_{59,59}$)		
	Original	Polynimal	Model
1	1.4335	1.5458	1.6926
2	1.1046	1.2271	3.2548
3	1.6961	2.5561	3.1550
4	1.6701	1.7248	2.1788
5	1.2970	1.3327	1.5098
6	1.1409	1.3153	1.4276
7	1.0064	1.6961	1.8957
8	1.0083	1.7504	2.3548

Table 1. F-statistics of assimilation with the original signal, assimilation after polynomial detrending, and detrend-free assimilation for the greatest activated area of the group in superior temporal gyrus (GTs). For a significance level of $P < 0.05$, $F_{0.95,59,59} = 1.54$.

generates better estimation of physiological states and reconstructed responses than separate processing (blue line). The statistical analysis effectively shows this case as well. It is noted that the significant level is greater by detrend-free assimilation ($F_{59,59} = 3.22$ for linear drift, $F_{59,59} = 2.51$ for quadratic drift, average from 250 simulations), which shows better detection performance in comparison with assimilation after polynomial detrending ($F_{59,59} = 3.00$ for linear drift, $F_{59,59} = 2.48$ for quadratic drift, average from 250 simulations).

Real Data. The real data was acquired from 8 healthy subjects. The condition for successive blocks alternated between rest and auditory stimulation, starting with additional 8 rest scans. Total 136 acquisitions were made (RT=2s), in blocks of 8, giving 16 16-second blocks. We select the largest activated voxels of the group in superior temporal gyrus (GTs) to implement assimilation.

Figure 2 (a), (b) show the real fMRI time series and the estimated drift by polynomial detrending method and the proposed method from two subjects. Intuitively, the estimated drift by detrend-free assimilation (blue line) can track the complicated drift variation with good approximation while the polynomial

approach (green line) does not work quite well. The estimated drift by detrend-free strategy has more freedom in selecting the structure of the drift component due to the introduction of physiological constraint. As a result, the detrend-free assimilation yields greater estimates of the fMRI response than separate processing (not presented here). Table 1 lists results of statistical analysis from all subjects. The statistic-F is obviously higher for detrend-free method than assimilation after polynomial detrending. In addition, in order to understand the effect of detrending on the spectrum of the fMRI signal, the power spectrum of the original time series is compared with detrended time series by the proposed method and polynomial method shown in Figure 2. It is noted that under the restriction of the hemodynamic model, detrend-free method has impact on all frequency contexts that are responsible to drift, whereas polynomial detrending only removes part of the low frequency component.

In this paper, we have developed a two-stage unscented estimator for nonlinear fMRI data assimilation, which casts the nonlinear unscented transform into the linear separate bias estimator, to account for the presence of time varying bias. It can deal with simultaneously the fMRI responses and drift in an assimilation cycle. It provides more accurate estimation of fMRI signal and physiological states than separate processing, thereby produces higher F value for statistic activation detection. On the other hand, it makes no assumption of the structure of the drift. As proper prior hemodynamics is adopted to guide the detrending procedure, information of the underlying physiological process is included, more reasonable drift estimates can be obtained. It is therefore particularly suited for fMRI imaging where the formulation of real drift remains difficult to acquire. Moreover, other prior knowledge can also be incorporated into the estimation procedure, such as cardiac and respiratory prior from external monitoring, and baseline drift of MR scanner.

Acknowledgments. This work is supported in part by the National Basic Research Program of China (2010CB732500) and in part by the National Natural Science Foundation of China (30800250).

References

1. Bazargani, N., Nasratinia, A., Gopinath, K., Briggs, R.W.: FMRI Baseline Drift Estimation Method by MDL Principle. In: 4th IEEE International Symposium on Biomedical Imaging (ISBI), Washington, D.C., USA, pp. 472–475 (2007)
2. Buxton, R.B., Wong, E.C., Frank, L.R.: Dynamics of Blood Flow and Oxygenation Changes During Brain Activation: The Balloon Model.. Magnetic Resonance in Medicine 39, 855–864 (1998)
3. Friedland, B.: Treatment of Bias in Recursive Filtering. IEEE Transactions on Automatic Control 14(4), 359–367 (1969)
4. Friston, K.J., Mechelli, A., Turner, R., Price, C.J.: Nonlinear Responses in fMRI: The Balloon Model, Volterra Kernels, and Other Hemodynamics.. NeuroImage 12, 466–477 (2000)
5. Hsieh, C.S.: General Two-stage Extended Kalman Filters. IEEE Transactions on Automatic Control 48(2), 289–293 (2003)

6. Hu, Z.H., Shi, P.C.: Nonlinear Analysis of BOLD Signal: Biophysical Modeling, Physiological States, and Functional Activation. In: Ayache, N., Ourselin, S., Maeder, A. (eds.) MICCAI 2007, Part II. LNCS, vol. 4792, pp. 734–741. Springer, Heidelberg (2007)
7. Hu, Z.H., Shi, P.C.: Sensitivity Analysis for Biomedical Models. IEEE Transactions on Medical Imaging 29(11), 1870–1881 (2010)
8. Julier, S.J., Uhlmann, J.K.: Unscented Filtering and Nonlinear Estimation. Proceeding of the IEEE 92(3), 401–422 (2004)
9. Moradkhani, H., Sorooshian, S., Gupta, H.V., Houser, P.R.: Dual State-parameter Estimation of Hydrological Models Using Ensemble Kalman Filter. Advance in Water Resouces 28, 135–147 (2005)